

LASERS

https://doi.org/10.1070/QEL16896

Control of the spectral parameters of neodymium ions in anisotropic crystals with a scheelite structure

G.V. Shilova, A.A. Sirotkin, P.G. Zverev

Abstract. **The spectral parameters of neodymium ions in anisotropic $YLiF_4$, $SrMoO_4$, $PbMoO_4$, $CaMoO_4$, $SrWO_4$, and $BaWO_4$ crystals with a scheelite structure are experimentally studied in the region of 1 μm. The luminescence spectra of neodymium ions at the $^4F_{3/2} \rightarrow {}^4I_{11/2}$ transition in these crystals exhibit pronounced polarisation dependences. It is shown that, using different orientations of the active laser element and separating a particular radiation polarisation, one can control the spectral dependence of the active medium gain, switch the laser wavelength, and create dual-wavelength lasers. A dual-wavelength $Nd^{3+}:YLiF_4$ laser emitting at λ = 1047 and 1053 nm with identical linear polarisations and good temporal and spatial matching is demonstrated.**

Keywords: *polarised luminescence spectrum, neodymium laser, anisotropic crystals, dual-wavelength lasing.*

1. Introduction

Neodymium-doped crystals serve as basic elements of numerous modern laser devices. The use of highly efficient semiconductor laser diodes as pump sources considerably extended the range of applicable laser materials. Of particular interest are anisotropic crystals, which make it possible to develop lasers whose wavelength depends on the radiation polarisation [1–7]. The emission spectrum of solid-state lasers is determined by the spectral-luminescent characteristics of the active medium. Most studies on lasing in anisotropic crystals use active laser elements cut so that the gain was maximal. The emission wavelength of lasers based on anisotropic crystals may change depending on the crystal orientation and the radiation polarisation. For example, lasers based on $Nd^{3+}:YVO_4$ crystals emit π-polarised radiation at λ = 1064 nm and σ-polarised radiation at λ = 1066 nm [6]. Orientation of vanadate crystals along different directions with respect to crystallographic axes allows one to considerably change the gain at one or another spectral component [7]. This, in turn, extends the functional capabilities of lasers based on vanadate crystals, namely, makes it possible to achieve wavelength tuning, to create dual-wavelength lasers with parallel or orthogonal polarisations of spectral components [8], extend the crystal gain spectrum, and achieve pico- and femtosecond laser pulses [9, 10].

G.V. Shilova, A.A. Sirotkin, P.G. Zverev A.M. Prokhorov General Physics Institute, Russian Academy of Sciences, ul. Vavilova 38, 119991 Moscow, Russia; e-mail: zverev@lst.gpi.ru

Received 9 November 2018; revision received 24 December 2018
Kvantovaya Elektronika **49** (6) 570–576 (2019)
Translated by M.N. Basieva

Solid-state lasers emitting simultaneously at two wavelengths have found practical applications in optical communication systems, environmental monitoring, remote probing, laser location, and medical equipment. For example, it was proposed in [11] to use dual-wavelength lasers to increase recording density in holographic interferometry. Intracavity generation of the sum frequency of a high-power dual-wavelength $Nd^{3+}:YAG$ laser provided narrow-band radiation at λ = 589 nm for creating artificial sodium stars [12]. Bruneau et al. [13] developed a two-wavelength alexandrite laser for determining atmospheric meteorological parameters. It is of great interest to obtain terahertz radiation by generating a difference frequency of a dual-wavelength laser with a small frequency shift between the spectral components [14]. Important requirements imposed on such lasers in many applications are good temporal and spatial matching of spectral components and their polarisation state.

The spectral characteristics of Nd^{3+} ions in crystals with a scheelite structure have a noticeable anisotropy. For example, the wavelength of lasers based on $Nd^{3+}:YLiF_4$ cut perpendicular to the $\boldsymbol{C}$ optical axis shifts from 1047 to 1053 nm as the π polarisation of laser radiation changes to the σ polarisation. The stimulated emission cross sections at these wavelengths are 1.8×10^{-19} and 1.2×10^{-19} cm^2, respectively [3]. These lasers usually emit at λ = 1047 nm. To obtain simultaneous dual-wavelength lasing, it is necessary to equalise the gains at the two spectral components. To do this, the authors of [15] used a dichroic output mirror with different reflection coefficients for two spectral components and obtained dual-wavelength laser radiation with two mutually perpendicular polarisations. An intracavity inclined glass plate was used in [16] to introduce spectrally- and polarisation-selective losses and achieve stable dual-wavelength lasing with different polarisations of components as well. The anisotropic physical properties of a lens-shaped $Nd^{3+}:YLF_4$ active element allowed the authors of [17] to control intracavity losses in a diode-pumped laser. To equalise the gain coefficients, it was proposed in [18] to use a $Nd^{3+}:YLF_4$ element cut at an angle of 50° to the optical axis. In this case, the stimulated emission cross sections at two wavelengths became identical for two mutually perpendicular polarisations, dual-wavelength lasing was obtained, and efficient difference frequency generation in the terahertz region was demonstrated. Note that all the dual-wavelength lasers described above emitted radiation with two mutually perpendicular polarisations.

The aim of the present work is to study the polarisation dependences of the luminescence spectra of Nd^{3+} ions at the $^4F_{3/2} \rightarrow {}^4I_{11/2}$ transition in anisotropic $YLiF_4$, $SrMoO_4$, $PbMoO_4$, $CaMoO_4$, $SrWO_4$ and $BaWO_4$ crystals, as well as to

study the possibility of using them for creating dual-wavelength lasers and to obtain lasing in a Nd^{3+}:$YLiF_4$ laser simultaneously at $\lambda = 1047$ and 1053 nm with identical linear polarisations.

2. Experimental setup and samples

The experimental optical scheme for studying the polarised luminescence spectra of samples depending on their orientation is shown in Fig. 1. The luminescence was excited by a LIMO HLU30F200 fibre-coupled diode laser, which emitted depolarised radiation at $\lambda = 808$ nm with a maximum power up to 30 W. The exciting radiation was focused into a spot with a diameter from 200 to 600 μm on a sample mounted on a holder rotatable in the plane perpendicular to the incident beam. The sample rotation angle was measured with an accuracy of 1°. An optical system consisting of two lenses and a Glan–Thompson prism separated one luminescence polarisation and directed the radiation to the input slit of a spectrometer. The luminescence spectrum was recorded using a multichannel spectrometer consisting of an UV-90 autocollimation tube (reciprocal linear dispersion 1.2 nm mm^{-1}) and a Toshiba TCD 1304JK CCD line array 30 mm in size connected to a computer. Luminescence spectra with different polarisations were recorded by rotating a sample under study by the angle $\alpha = 0–360°$ with a step of 10°. The samples of Nd^{3+}:$YLiF_4$, Nd^{3+}:$SrMoO_4$, Nd^{3+}:$CaMoO_4$, Nd^{3+}:$PbMoO_4$, Nd^{3+}:$SrWO_4$, and Nd^{3+}:$BaWO_4$ crystals were cut perpendicular to the $\boldsymbol{C}$ optical axis. The length of the samples varied from 8 to 40 mm. Rotation of samples made it possible to record π-polarised ($\boldsymbol{E} \| \boldsymbol{C}$, $\alpha = 0°$) and σ-polarised ($\boldsymbol{E} \perp \boldsymbol{C}$, $\alpha = 90°$) luminescence, as well as spectra at arbitrary crystal rotation angles α.

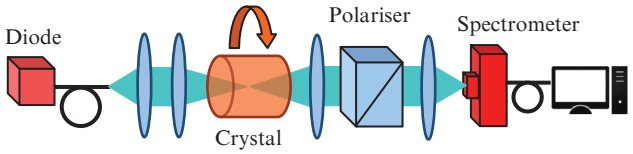

Figure 1. Experimental optical scheme for measuring polarisation dependences of luminescence spectra of Nd^{3+} ions in crystals.

3. Study of polarisation dependences of Nd^{3+} luminescence at the $^4F_{3/2} \rightarrow {}^4I_{11/2}$ transition

In the general case, the luminescence spectrum of Nd^{3+} ions in crystals at the $^4F_{3/2} \rightarrow {}^4I_{11/2}$ transition in the range of 1.04–1.08 μm consists of 12 lines corresponding to transitions between different Stark components, i.e., two components of the upper $^4F_{3/2}$ level (R_1 and R_2) and six components of the lower $^4I_{11/2}$ level (Y_1–Y_6). The intensity and frequency of individual lines are determined by the influence of the local crystal field on the Nd^{3+} ion and are related to the crystal structure. At room temperature, individual lines in the luminescence spectra may overlap and form a total spectrum consisting of rather broad bands. The intensity of individual lines (bands) in anisotropic crystals depends on the recorded radiation polarisation.

3.1. Polarisation dependences of Nd^{3+} luminescence in Nd^{3+}:$YLiF_4$ crystals

Nd^{3+}:$YLiF_4$ crystals have a number of advantages for developing diode-pumped lasers. The lifetime of Nd^{3+} ions in these crystals is twice as long as in Nd^{3+}:YAG, which allows formation of high population inversion in the active material. The $YLiF_4$ crystal has a scheelite-like structure, which leads to anisotropy of its optical properties. Let us consider the energy level diagram and the luminescence spectrum of Nd^{3+} ions at the $^4F_{3/2} \rightarrow {}^4I_{11/2}$ transition in $YLiF_4$ crystals in more detail (Figs. 2, 3). One can see that the wavelengths of luminescence peaks well agree with the energies of the corresponding levels. Note that the level with an energy of 2042 cm^{-1} is doubly degenerate (Y_2, Y_3) and some transitions have close wavelengths, which decreases the total number of luminescence peaks to seven (see Fig. 3).

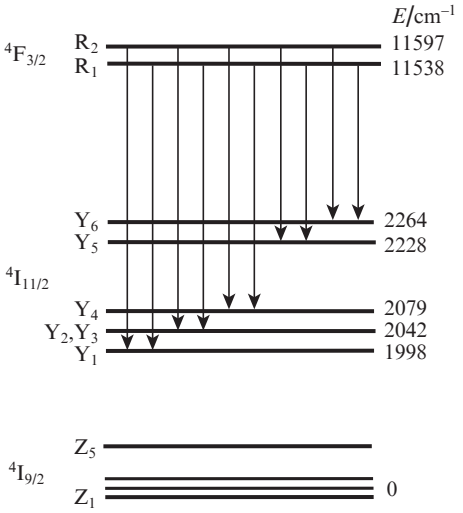

Figure 2. Energy level diagram and $^4F_{3/2} \rightarrow {}^4I_{11/2}$ transitions in Nd^{3+}:$YLiF_4$ crystal [19].

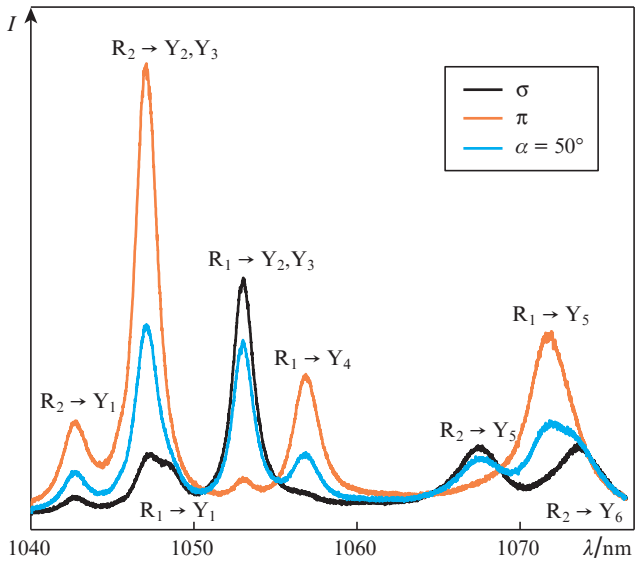

Figure 3. (Colour online) Luminescence spectra of Nd^{3+} ions at the $^4F_{3/2} \rightarrow {}^4I_{11/2}$ transition in Nd^{3+}:$YLiF_4$ crystal for different polarisations.

The intensities of the spectral lines depend on the polarisation of the recorded radiation. The luminescence line at $\lambda = 1047.1$ nm is most intense in the case of π polarisation and almost disappears in the spectrum of σ-polarised luminescence. At the same time, the intense σ-polarised luminescence line

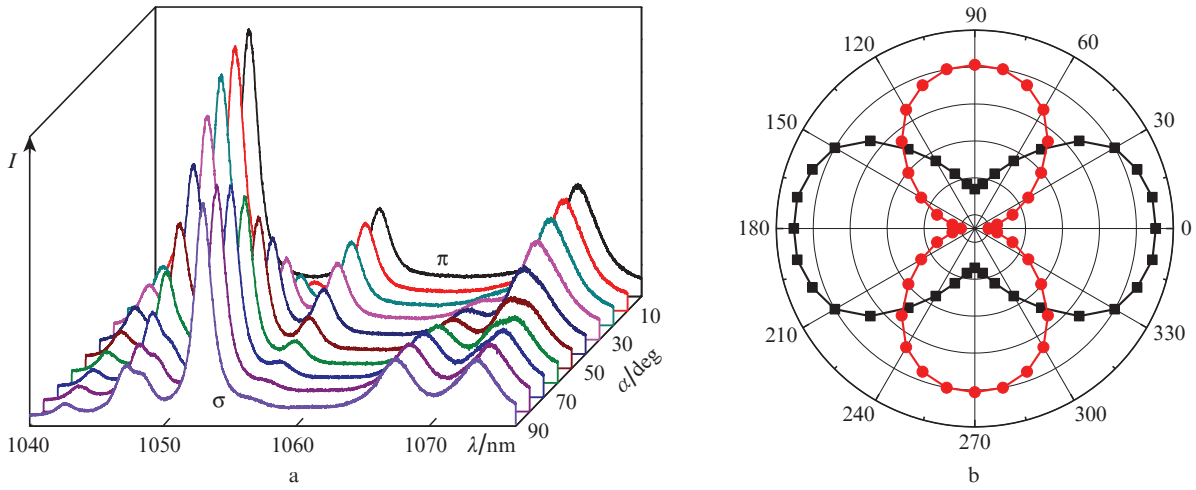

Figure 4. (Colour online) (a) Luminescence spectra of a $Nd^{3+}:YLiF_4$ crystal for different polarisations of recorded radiation with respect to the crystal axes and (b) polar diagram of intensities of spectral peaks at λ = (■) 1047.1 and (●) 1053 nm.

at λ = 1053 is almost absent in the spectrum of π-polarised luminescence. When the sample is rotated by the angle $\alpha = 50°$, the amplitudes of the luminescence peaks at λ = 1047.1 and 1053 nm become close to each other. Figure 4a shows a more informative pattern of the luminescence spectrum transformation depending on the crystal rotation angle in the range α = 0–90°. Figure 4b presents the dependences of intensities of the luminescence peaks at λ = 1047.1 and 1053 on the crystal rotation angle in the range from 0 to 360 in polar coordinates. The rotation angle of 0° (180°) corresponds to the π polarisation.

One can see that, by cutting crystals at some angles and selecting a particular polarisation of radiation, one can control the spectral parameters of the $Nd^{3+}:YLiF_4$ active crystal, considerably change the gain cross section at particular wavelengths and the shape of the gain spectra, and tune the laser wavelength. At the points of intersection of the curves in Fig. 4b corresponding to the crystal rotation angles α = 50°, 130°, 230°, and 310°, the intensities of lines at λ = 1047.1 and 1053 nm become equal. This testifies to identical gains at these wavelengths for radiation with the given polarisation, i.e., to the possibility of dual-wavelength lasing with one polarisation.

3.2. Polarisation dependences of Nd^{3+} luminescence in $SrMoO_4$, $PbMoO_4$, $CaMoO_4$, $SrWO_4$, and $BaWO_4$ crystals

Molybdate and tungstate crystals with the scheelite structure (general formula MXO_4, where M = Ca, Sr, Ba, Pb and X = W, Mo) belong to uniaxial nonlinear optical SRS-active crystals with a high cubic nonlinear susceptibility. Their crystal structure allows doping with rare-earth (RE) ions, which makes these crystals promising laser materials. However, substitution of divalent M^{2+} cations by trivalent RE ions requires charge compensation by codoping with additional impurities [20, 21], which leads to inhomogeneous broadening of the spectral lines of RE ions. Below we consider in more detail the luminescent characteristics of Nd^{3+} ions in molybdate and tungstate crystals with the scheelite structure.

Lasing in a $Nd^{3+}:SrMoO_4$ crystal was achieved as early as in 1963 [22]. The authors of [20] observed switching of the wavelength of a pulse-pumped laser from 1057.6 to 1064.3 nm as the crystal temperature decreased from 295 to 77 K. Later, it was found that $SrMoO_4$ crystals are promising as SRS-

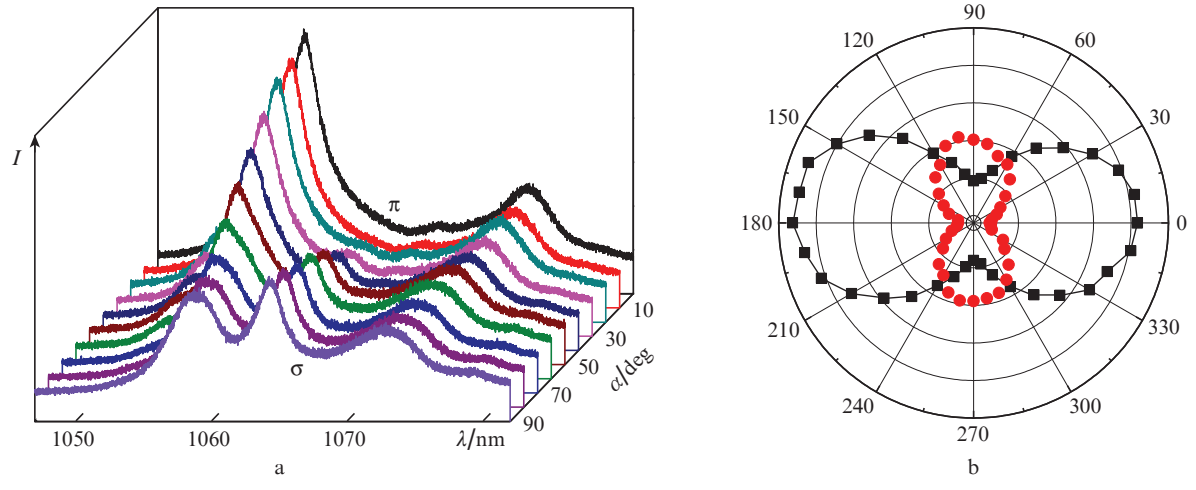

Figure 5. (Colour online) (a) Luminescence spectra of Nd^{3+} ions in a $Nd^{3+}:SrMoO_4$ crystal for different crystal orientations and (b) polar diagram of intensities of peaks at λ = (■) 1057.7 and (●) 1064.7 nm.

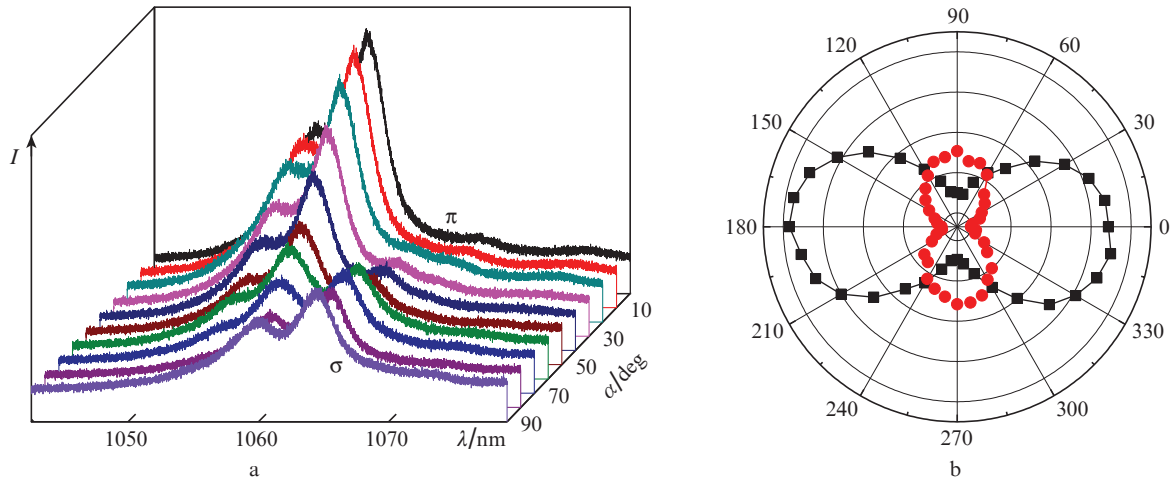

Figure 6. (Colour online) (a) Luminescence spectra of Nd^{3+} ions in a $Nd^{3+}:PbMoO_4$ crystal for different crystal orientations and (b) polar diagram of peak intensities at λ = (■) 1058.8 and (●) 1064.4 nm.

active materials [23], while Nd^{3+}-doped crystals can be used as multifunctional active and nonlinear materials in diode-pumped solid-state Raman lasers [24, 25].

Figure 5a shows the luminescence spectra for different orientations of a $Nd^{3+}:SrMoO_4$ crystal. The width of the most intense line is 3.5 nm, which is considerably larger than that in $Nd^{3+}:YLiF_4$. The spectra contain three main lines, at λ = 1057.7, 1064.7, and 1073.0 nm. The most intense lines in the π- and σ-polarised luminescence spectra lie at λ = 1057.7 and 1064.7 nm, respectively. In the case of the crystal rotation angle α = 60°, the intensities of these lines become identical (Fig. 5b) and identical gains at these wavelengths make possible dual-wavelength lasing in the $Nd^{3+}:SrMoO_4$ crystal.

The $PbMoO_4$ crystal is also known as an efficient acousto-optic material with an extremely high cubic nonlinearity [26]. Lasing in a $Nd^{3+}:PbMoO_4$ crystal was observed at λ = 1058.6 nm [22, 27]. The crystal anisotropy leads to a change in the luminescent properties of Nd^{3+} ions in the region of 1 μm depending on the sample orientation. Figure 6a presents the luminescence spectra for a $Nd^{3+}:PbMoO_4$ crystal. The spectral width of the laser transition for the π polarisation is 4.3 nm, while the Stark splitting is somewhat smaller than in the other studied crystals. The π- and σ-polarised luminescence lines with the maximum intensity lie at 1058.8 and 1064.4 nm, respectively. Similar to strontium molybdate, the intensities of these peaks become identical in the case of the crystal rotation by α = 60° (Fig. 6b).

Lasing in a $Nd^{3+}:CaMoO_4$ crystal was observed at λ = 1059.5 and 1067 nm [20, 22]. The possibility of switching the laser wavelength by changing the laser radiation polarisation was observed in [28]. The luminescence spectrum of Nd^{3+} ions in the $Nd^{3+}:CaMoO_4$ crystal exhibits nine Stark components, which cover the spectral range from 1055 to 1084 nm (Fig. 7a). The maximum intensity in the π-polarised luminescence spectrum belongs to the line at λ = 1067.1 nm. The σ-polarised luminescence spectrum contains two lines with identical intensities at λ = 1060 and 1081.9 nm. At the crystal rotation angle α = 45°, the intensities of the three lines become identical and the luminescence spectrum represents a weakly structured band 30 nm wide, which makes it possible to use this crystal as an active medium of subpicosecond lasers.

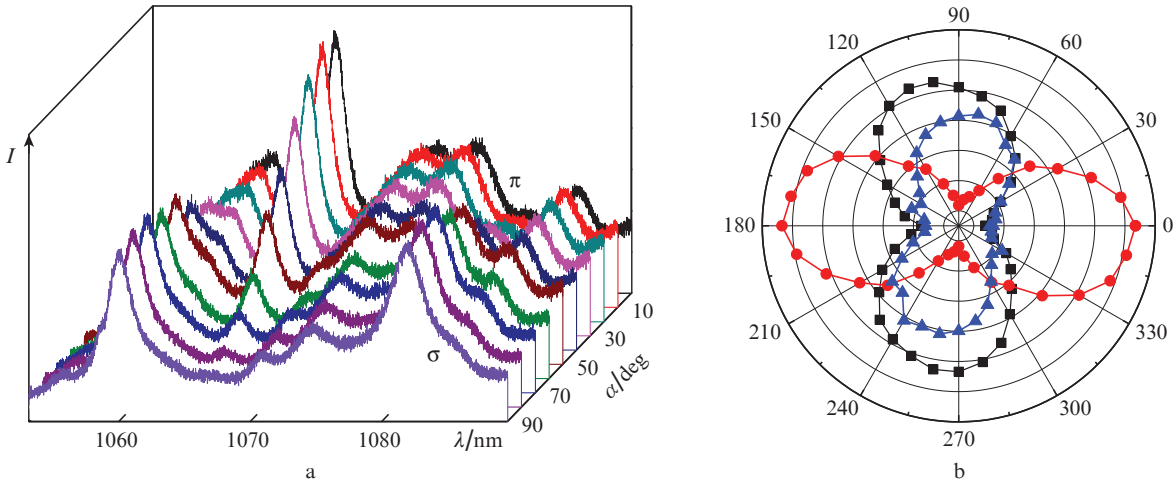

Figure 7. (Colour online) (a) Luminescence spectra of Nd^{3+} ions in a $Nd^{3+}:CaMoO_4$ crystal for different crystal orientations and (b) polar diagram of peak intensities at λ = (■) 1060, (●) 1067.1, and (▲) 1081.9 nm.

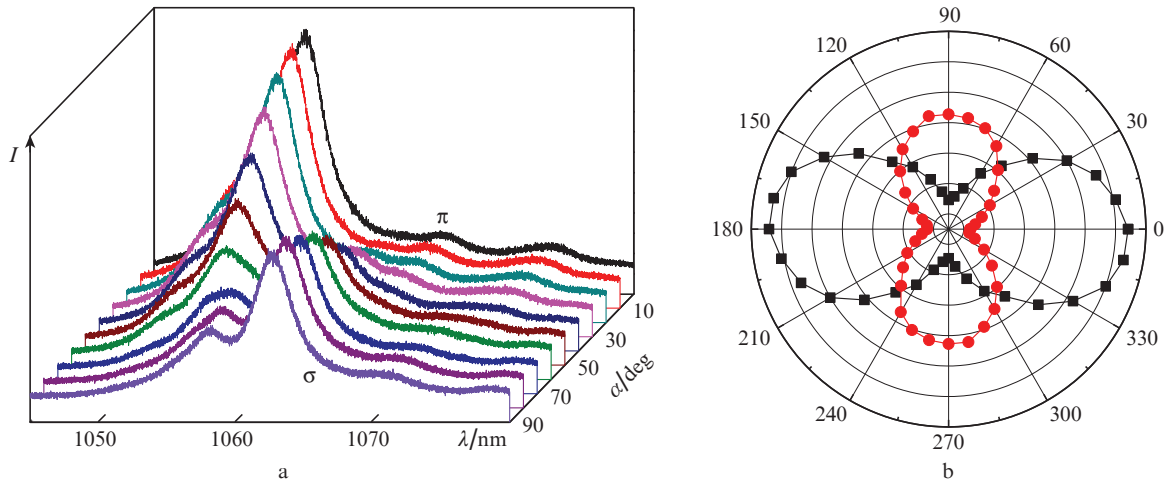

Figure 8. (Colour online) (a) Luminescence spectra of Nd^{3+} ions in a $Nd^{3+}:SrWO_4$ crystal for different crystal orientations and (b) polar diagram of peak intensities at λ = (■) 1056.0 and (●) 1063.5 nm.

Lasing in a $Nd^{3+}:SrWO_4$ crystal at the $^4F_{3/2} \rightarrow {}^4I_{11/2}$ transition was previously observed at λ = 1057 and 1063 nm [22, 27]. Figure 8a shows the luminescence spectra of a $Nd^{3+}:SrWO_4$ crystal for different polarisations. One can see that the dominant line in the π-polarised luminescence spectrum lies at λ = 1056.0 nm and has a spectral width of 4.7 nm. The maximum intensity in the σ-polarised luminescence spectrum is observed at λ = 1063.5 nm. At the crystal rotation angle α = 45°, the intensities of these lines become equal to each other (Fig. 8b) and the $Nd^{3+}:SrWO_4$ laser can emit at two frequencies.

Note that not all scheelite-like crystals demonstrate wavelength switching as the polarisation changes from π- to σ-type. Figure 9 presents the luminescence spectra of a $Nd^{3+}:BaWO_4$ crystal for different orientations. Only one line with λ = 1055.0 nm and a spectral width of ~4.9 nm dominates in all spectra. The intensity of this line is maximum for the π polarisation and decreases in the case of the σ polarisation, which was observed in laser experiments [29]. This polarisation dependence of luminescence spectra is obviously related to a specific feature of the $BaWO_4$ crystal structure responsible for a weaker anisotropy of the crystal field affecting Nd^{3+} ions than in the other studied crystals. This is confirmed, in particular, by the minimal difference between the n_o and n_e refractive indices of the $BaWO_4$ crystal among all the considered crystals [21].

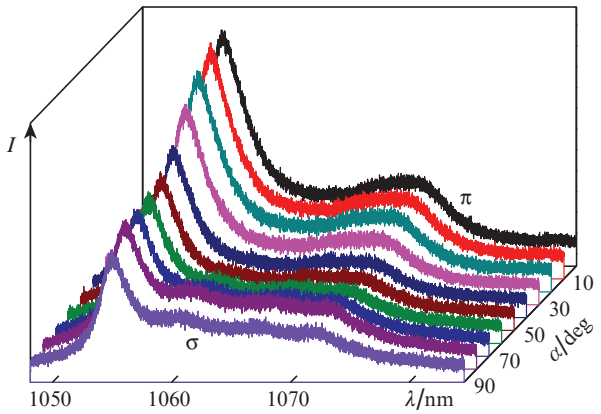

Figure 9. (Colour online) Luminescence spectra of Nd^{3+} ions in a $Nd^{3+}:SrWO_4$ crystal for different crystal orientations.

Table 1 lists the results of our investigations, namely, wavelengths of luminescence peaks with different polarisations, orientations of crystals for creating a dual-wavelength laser with identical polarisations of the spectral components, and the calculated laser frequency in the terahertz region that can be obtained by difference frequency generation in a nonlinear crystal. Table 1 shows that, using one or another active material, it is possible to create terahertz sources in the frequency range of 1.46–3.87 THz. Note that, although the studied crystals are isostructural, they considerably differ by ionic radii or by anionic complexes. This leads to different crystal lattice parameters, as well as to different strengths and anisotropy of their crystal fields. As a result, their luminescence spectra exhibit different Stark splittings of the levels of Nd^{3+} ions, which causes a frequency shift of luminescence peaks and a change in their intensities. In general, the structures of Nd^{3+} levels responsible for the $^4F_{3/2} \rightarrow {}^4I_{11/2}$ transition in the studied crystals are similar. Because of this, the orientation of these crystals required for dual-wavelength lasing differs insignificantly.

Table 1. Wavelengths of π- and σ-polarised luminescence peaks of Nd^{3+} ions in the studied crystal, orientations of crystals for achieving identical intensities of these lines and for creating dual-wavelength lasers, and calculated difference frequency in the terahertz region.

Crystal	Peak wavelength/nm	Crystal orientation/deg	Difference frequency/THz
$Nd^{3+}:YLiF_4$	1047.1 (π)	50	1.61
	1053.0 (σ)		
$Nd^{3+}:SrMoO_4$	1057.7 (π)	60	1.86
	1064.7 (σ)		
$Nd^{3+}:CaMoO_4$	1060.0 (π)	45	1.88
	1067.1 (σ)		3.85
	1081.9 (σ)		
$Nd^{3+}:PbMoO_4$	1058.8 (π)	60	1.49
	1064.4 (σ)		
$Nd^{3+}:SrWO_4$	1056.0 (π)	45	2.00
	1063.5 (σ)		
$Nd^{3+}:BaWO_4$	1055.0 (π)	–	–
	1055.0 (σ)		

4. Dual-wavelength $Nd^{3+}:YLiF_4$ crystal laser with linear polarisation

To obtain dual-wavelength lasing with identical linear polarisations of generated components, we used a lamp-pumped $Nd^{3+}:YLiF_4$ laser. An active element 7 mm in diameter and 90 mm long was placed in a K-301 laser head with an INP 6/90 pulsed lamp. The 45-nm cavity consisted of two plane mirrors (Fig. 10). The reflection coefficient of the output mirror in the case of the free-running mode ($R_{1.04-1.06}$) was 62%. An antireflection-coated Glan prism between the active element and the highly-reflecting mirror determined the laser radiation polarisation. To achieve a Q-switching regime, we used an electro-optic Q-switch based on a DKDP crystal 20 mm long and an output mirror with $R_{1.04-1.06}$ = 41%. The laser spectrum was recorded using an Ocean Optics spectrometer and processed with SpectraSuite software. The laser operated in the repetitively pulsed regime with a pulse repetition rate of 5 Hz. Rotating the Glan prism between the positions corresponding to the transmission of π and σ polarisations, we observed changes in the polarisation and intensity of the output radiation, as well as wavelength switching from 1047.1 to 1053 nm. At the intermediate rotation angle α = 50°, lasing occurred simultaneously at two wavelengths with a linear polarisation. The maximum output energy in the free-running mode was observed in the case of the π polarisation and λ = 1047.1 nm (Fig. 11), which is explained by a higher stimulated emission cross section [3]. In the dual-wavelength regime at a pump energy of 95 J, the laser generated

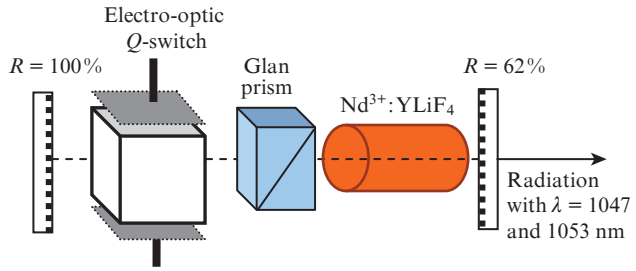

Figure 10. Optical scheme of a dual-wavelength $Nd^{3+}:YLiF_4$ laser.

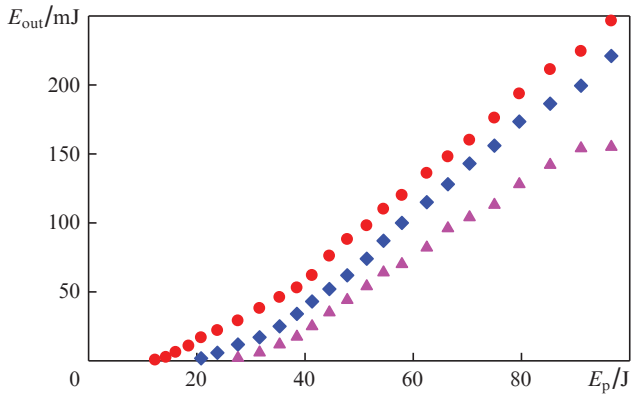

Figure 11. Dependences of the output energy of a $Nd^{3+}:YLiF_4$ laser on the pump energy for the free-running mode with (●) π-polarised radiation at λ = 1047.1 nm and (◆) σ-polarised radiation at λ = 1053 nm, as well as (▲) in the dual-wavelength regime with a linear polarisation at a Glan prism rotation angle of 50°.

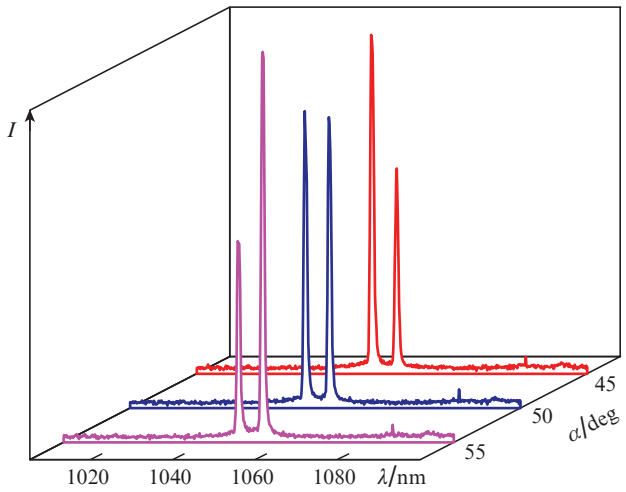

Figure 12. Spectra of a $Nd^{3+}:YLiF_4$ laser in the free-running mode at rotation of the intracavity Glan prism by angles of 45°, 50°, and 55°.

linearly polarised radiation at two wavelengths with identical energies of 160 mJ (Fig. 12). Rotation of the polariser by 5° caused redistribution between the energies of the spectral components (see Fig. 12).

In the case of the Q-switching regime with the use of a DKDP quarter-wave electrooptic Q-switch, rotation of the active element by the angle α = 50° with respect to the polariser plane allowed us to achieve dual-wavelength lasing with a pulse energy of 32 mJ at a pulse duration of 25 ns. It should be noted that, due to identical intracavity losses at the two wavelengths, gain coefficients at these wavelengths are also identical and lasing develops simultaneously. This made it possible to achieve efficient sum-frequency generation in a $LiIO_3$ crystal at a wavelength of 525 nm, which confirmed good temporal and spatial matching of the spectral components of the dual-wavelength laser.

5. Conclusions

Polarisation dependences of the luminescence spectra of Nd^{3+} ions at the $^4F_{3/2} \rightarrow {}^4I_{11/2}$ transition in anisotropic $YLiF_4$, $SrMoO_4$, $PbMoO_4$, $CaMoO_4$, $SrWO_4$, and $BaWO_4$ crystals with the scheelite structure are studied experimentally. It is shown that, using different orientations of the active laser element and separating a particular polarisation in the generated radiation, it is possible to control the spectral dependence of the active medium gain, switch the laser wavelength, and develop dual-wavelength lasers. For $Nd^{3+}:YLiF_4$, $Nd^{3+}:SrMoO_4$, $Nd^{3+}:PbMoO_4$, $Nd^{3+}:CaMoO_4$, and $Nd^{3+}:SrWO_4$ crystals, the polarisation orientations with respect to the crystal optical axis at which the luminescence intensities become identical for two wavelengths are determined, which makes it possible to use these crystals for developing dual-wavelength lasers with linear polarisation. A laser based on a $Nd^{3+}:YLiF_4$ crystal emitting at λ = 1047.1 and 1053 nm with identical linear polarisation and good temporal and spatial matching is demonstrated for the first time.

Acknowledgements. The authors thank L.I. Ivleva (A.M. Prokhorov General Physics Institute, Russian Academy of Sciences) for providing samples of neodymium-doped strontium and calcium tungstate and molybdate crystals.

References

1. Morozov A.M., Tolstoi M.N., Feofilov P.P. *Opt. Spectrosc.*, **22**, 139 (1967) [*Opt. Spektrosk.*, **22**, 258 (1967)].
2. Weber M.J., Varitimos T.E. *J. Appl. Phys.*, **42** (12), 4996 (1971).
3. Frei B., Balmer J.E. *Appl. Opt.*, **33** (30), 6942 (1994).
4. Šulc J., Jelınkova H., Basiev T.T., Doroschenko M.E., Ivleva L.I., Osiko V.V., Zverev P.G. *Opt. Mater.*, **30**, 195 (2007).
5. Chen Y.F. *Appl. Phys. B*, **70** (4), 475 (2000).
6. Vlasov V.I., Garnov S.V., Zavartsev Yu.D., Zagumennyi A.I., Kutovoi S.A., Sirotkin A.A., Shcherbakov I.A. *Quantum Electron.*, **37** (10), 938 (2007) [*Kvantovaya Elektron.*, **37** (10), 938 (2007)].
7. Sirotkin A.A., Vlasov V.I., Zagumennyi A.I., Zavartsev Yu.D., Kutovoi S.A., Shcherbakov I.A. *Quantum Electron.*, **44** (1), 7 (2014) [*Kvantovaya Elektron.*, **44** (1), 7 (2014)].
8. Sirotkin A.A., Garnov S.V., Vlasov V.I., Zagumennyi A.I., Zavartsev Yu.D., Kutovoi S.A., Shcherbakov I.A. *Quantum Electron.*, **42** (5), 420 (2012) [*Kvantovaya Elektron.*, **42** (5), 420 (2012)].
9. Sirotkin A.A., Sadovskii S.P., Garnov S.V. *Quantum Electron.*, **43** (7), 600 (2013) [*Kvantovaya Elektron.*, **43** (7), 600 (2013)].
10. Sirotkin A.A. *Prikl. Spektrosk.*, **83** (6–16), 588 (2016).
11. Weigl F. *Appl. Opt.*, **10** (1), 187 (1971).
12. Bienfang J.C., Denman C.A., Grime B.W., Hillman P.D., Moore G.T., Telle J.M. *Opt. Lett.*, **28** (22), 2219 (2003).
13. Bruneau D., Cazeneuve H., Loth C., Pelon J. *Appl. Opt.*, **30** (27), 3930 (1991).
14. Zhao P., Ragam S., Ding Y.J., Zotova I.B. *Opt. Lett.*, **36** (24), 4818 (2011).
15. Lin Z., Wang Y., Xu B., Cheng Y., Xu H., Cai Z. *Opt. Eng.*, **54** (12), 126114 (2015).
16. Zhang J., Liu H.L., Xia J., Fu X. *Chin. Opt. Lett.*, **13** (3), 031402 (2015).
17. Bezotosnyi V.V., Gorbunkov M.V., Kostryukov P.V., Popov Yu.M., Tunkin V.G., Cheshev E.A. *Bull. Lebedev Phys. Inst.*, **38** (10), 311 (2011) [*Kratk. Soobshch. Fiz. FIAN*, **38** (10), 43 (2011)].
18. Brenier A. *Opt. Lett.*, **40** (19), 4496 (2015).
19. Chuang T., Verdun H.R. *IEEE J. Quantum Electron.*, **32** (1), 79 (1996).
20. Flournoy P.A., Brixner L.H. *J. Electrochem. Soc.*, **112** (8), 779 (1965).
21. Voronina I.S., Ivleva L.I., Basiev T.T., Zverev P.G., Polozkov N.M. *J. Optoelectron. Adv. Mater.*, **5** (4), 887 (2003).
22. Zverev P.G., Karasik A.Ya., Basiev T.T., Ivleva L.I., Osiko V.V. *Quantum Electron.*, **33** (4), 331 (2003) [*Kvantovaya Elektron.*, **33** (4), 331 (2003)].
23. Doroshenko M.E., Basiev T.T., Vassiliev S.V., Ivleva L.I., Komar V.K., Kosmyna M.B., Kosmyna M.B., Jelinkova H., Šulc J. *Opt. Mater.*, **30** (1), 54 (2007).
24. Basiev T.T., Doroshenko M.E., Ivleva L.I., Voronina I.S., Konjushkin V.A., Osiko V.V., Vasilyev S.V. *Opt. Lett.*, **34** (7), 1102 (2009).
25. Basiev T.T., Zverev P.G., Karasik A.Ya., Osiko V.V., Sobol A.A., Chunaev D.S. *JETP*, **126** (5), 934 (2004) [*Zh. Eksp. Teor. Fiz.*, **126** (5), 1073 (2004)].
26. Johnson L.F. *J. Appl. Phys.*, **34** (4), 897 (1963).
27. Basiev T.T., Doroshenko M.E., Ivleva L.I., Osiko V.V., Kosmyna M.B., Komar' V.K., Šulc J., Jelinkova H. *Quantum Electron.*, **36** (8), 720 (2006) [*Kvantovaya Elektron.*, **36** (8), 720 (2006)].
28. Blistanov A.A., Galagan B.I., Denker B.I., Ivleva L.I., Osiko V.V., Polozkov N.M., Sverchkov Yu.E. *Sov. J. Quantum Electron.*, **19**, 747 (1989) [*Kvantovaya Elektron.*, **16** (6), 1152 (1989)].
29. Šulc J., Jelínkova H., Basiev T.T., Doroschenko M.E., Ivleva L.I., Osiko V.V., Zverev P.G. *Proc. SPIE*, **6100**, 61000Z (2006).